Articles

High-Temperature and Long-Term Stable Solid-State Electrolyte for Dye-Sensitized Solar Cells by Self-assembly

Hong Yang,[†] Chengzhong Yu,[†] Qunliang Song,[‡] Yongyao Xia,[†] Fuyou Li,*[,†] Zhigang Chen,[†] Xianghong Li,[†] Tao Yi,[†] and Chunhui Huang*[,†]

Department of Chemistry & Laboratory of Advanced Materials, and National Key Laboratory of Surface Physics, Fudan University, Shanghai 200433, P. R. China

Received May 12, 2006. Revised Manuscript Received August 4, 2006

Ionic liquid 1-butyl-3-methylimidazolium tetrafluoroborate was solidified by silica nanoparticles (>2 wt %) even up to 85 °C. The mechanism of solid-state composites was inferred to self-assemble through hydrogen bond networks between the anion BF_4^- and the hydroxyl group in the surface of silica nanoparticles, which was characterized by differential scanning calorimetry measurement and Fourier transition infrared spectra. The solid-state composite was introduced to form high-temperature solid-state electrolytes for highly efficient dye-sensitized solar cells with an overall energy-conversion efficiency of 4.7% at room temperature and 5.0% at 60 °C under AM 1.5 sunlight illumination (75 mW cm^{-2}).

Introduction

Dye-sensitized nanocrystalline solar cells (DSSCs) have aroused considerable attention due to their high-energy conversion efficiency and especially low production cost as cheaper alternatives to silicon solar cells.[1−3] At present, practical problems such as leakage and evaporation of organic solvent become serious obstacles to the application of DSSCs.[4] Therefore, it is important to develop solid-state electrolytes, especially for improving the stability of DSSCs. Several attempts have been made to substitute solid-state electrolytes (such as polymer electrolytes,[5−8] plastic crystal electrolytes,[9] organic hole-transport materials,[10,11] and inorganic semiconductors[12−14]) for liquid electrolytes.

Since the temperature of solar cells may reach 60 °C under full sunlight, it is necessary that DSSCs maintain high overall energy conversion efficiency (>4%) under natural conditions.[4] Up to now, the reported solid-state DSSCs with an overall energy conversion efficiency beyond 4% exhibit the highest melting point of only 52 °C.[8c] Therefore, it is still a challenge to design a high-temperature (>60 °C) solid-state DSSC with high efficiency (>4%).

Because of the relatively high ionic conductivity and low viscosity,[15] room-temperature ionic liquid (RTIL) was widely used in DSSCs as a solvent and an important source for iodide-based redox couple.[16] To reduce the fluidity of RTIL-based electrolytes, several strategies have been proposed by incorporating small molecular organogels[17] and SiO_2 nanoparticles.[18] Recently, Grätzel et al. have reported that ionic

* Authors to whom correspondence should be addressed. E-mail: fyli@fudan.edu.cn; chhuang@pku.edu.cn. Tel.: 86-21-55664185. Fax: 86-21-55664621.

[†] Department of Chemistry & Laboratory of Advanced Materials.

[‡] National Key Laboratory of Surface Physics.

(1) (a) Grätzel, M. *Nature* **2001**, *414*, 338. (b) Schmidt-Mende, L.; Bach, U.; Humphry-Baker, R.; Horiuchi, T.; Miura, H.; Ito, S.; Uchida, S.; Grätzel, M. *Adv. Mater.* **2005**, *17*, 813.

(2) (a) Adachi, M.; Murata, Y.; Takao, J.; Jiu, J.; Sakamoto, M.; Wang, F. *J. Am. Chem. Soc.* **2004**, *126*, 14943. (b) Sayama, K.; Tsukagoshi, S.; Hara, K.; Ohga, Y.; Shinpou, A.; Abe, Y.; Suga, S.; Arakawa, H. *J. Phys. Chem. B* **2002**, *106*, 1363. (c) Hara, K.; Kurashige, M.; Ito, S.; Shinpo, A.; Suga, S.; Sayama, K.; Arakawa, H. *Chem. Commun.* **2003**, 252.

(3) (a) Wang, Z. S.; Li, F. Y.; Huang, C. H. *J. Phys. Chem. B* **2001**, *105*, 9210. (b) Hou, K.; Tian, B. Z.; Li, F. Y.; Bian, Z. Q.; Zhao, D. Y.; Huang, C. H. *J Mater. Chem.* **2005**, *15*, 2414.

(4) Grätzel, M. *J. Photochem. Photobiol. A* **2004**, *164*, 3.

(5) (a) Stergiopoulos, T.; Arabatzis, I. M.; Katsaros, G.; Falaras, P. *Nano Lett.* **2002**, *2*, 1259. (b) Stergiopoulos, T.; Arabatzis, I. M.; Cachet, H.; Falaras, P. *J. Photochem. Photobiol. A* **2003**, *155*, 163.

(6) (a) Nogueira, A. F.; Durrant, J. R.; De Paoli, M. A. *Adv. Mate*r. **2001**, *13*, 826. (b) Longo, C.; Nogueira, A. F.; De Paoli, M. A.; Cachet, H. *J. Phys. Chem. B* **2002**, *106*, 5925.

(7) (a) Wang, P.; Zakeeruddin, S. M.; Exnar, I.; Grätzel, M. *Chem. Commun.* **2002**, 2972. (b) Wang, H. X.; Li, H.; Xue, B. F.; Wang, Z. X.; Meng, Q. B.; Chen, L. Q. *J. Am. Chem. Soc.* **2005**, *127*, 6394.

(8) (a) Kim, Y. J.; Kim, J. H.; Kang, M. S.; Lee, M. J.; Won, J.; Lee, J. C.; Kang, Y. S. *Adv. Mater.* **2004**, *16*, 1753. (b) Kang, M. S.; Kim, J. H.; Kim, Y. J.; Won, J.; Park, N. G.; Kang, Y. S. *Chem. Commun.* **2005**, 889. (c) Han, H. W.; Liu, W.; Zhang, J.; Zhao, X. Z. *Adv. Funct. Mater.* **2005**, *15*, 1940.

(9) Wang, P.; Dai, Q.; Zakeeruddin, S. M.; Forsyth, M.; MacFarlane, D. R.; Grätzel, M. *J. Am. Chem. Soc.* **2004**, *126*, 13590.

(10) (a) Bach, U.; Lupo, D.; Comte, P.; Moser, J. E.; Weissortel, F.; Salbeck, J.; Spreitzer, H.; Grätzel, M. *Nature* **1998**, *395*, 583. (b) Haridas, K. R.; Ostrauskaite, J.; Thelakkat, M.; Heim, M.; Bilke, R.; Harrer, D. *Synth. Met.* **2001**, *121*, 1573.

(11) (a) Ikeda, N.; Miyasaka, T. *Chem. Commun.* **2005**, 1886. (b) Schmidt-Mende, L.; Kroeze, J. E.; Durrant, J. R.; Nazeeruddin, M. K.; Grätzel, M. *Nano Lett.* **2005**, *5*, 13150.

(12) (a) Kumara, G. R. A.; Kaneko, S.; Okuya M.; Tennakone, K. *Langmuir* **2002**, *18*, 10493. (b) Kumara, G. R. A.; Konno, A.; Shiratsuchi, K.; Tsukahara, J.; Tennakone, K. *Chem. Mater.* **2002**, *14*, 954. (c) Perera, V. P. S.; Pitigala, P. K. D. D. P.; Jayaweera, P. V. V.; Bandaranayake, K. M. P.; Tennakone, K. *J. Phys. Chem. B* **2003**, *107*, 13758.

(13) Tan, S. X.; Zhai, J.; Wan, M. X .; Meng, Q. B.; Li, Y. L.; Jiang, L.; Zhu, D. B. *J. Phys. Chem. B* **2004**, *108*, 18693.

(14) O'Regan, B.; Schwartz, D. T. *Chem. Mater.* **1998**, *10*, 1501.

(15) Dupont, J.; De Souza, R. F.; Suarez, P. A. Z. *Chem. Rev.* **2002**, *102*, 3667, and references therein.

10.1021/cm061112d CCC: $33.50 © 2006 American Chemical Society
Published on Web 10/04/2006

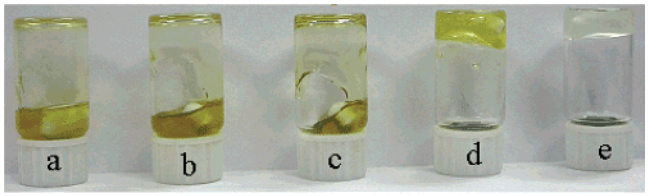

Figure 1. Photographs of the mixture of ionic liquid and SiO_2 nanoparicles: (a) BMI·I−SiO_2 (5 wt %), (b) BMI·I−BMI·BF_4 (3:1, v/v)−SiO_2 (5 wt %), (c) BMI·I− BMI·BF_4 (1:1, v/v)−SiO_2 (5 wt %), (d) BMI·I−BMI·BF_4 (1:3, v/v)−SiO_2 (5 wt %), (e) BMI·BF_4−SiO_2 (5 wt %) at room temperature.

liquid-based quasi-solid-state electrolytes were successfully employed for DSSC with the highest efficiency of 7% at AM 1.5 sunlight in combination with an amphiphilic ruthenium polypyridyl photosensitizer.[18] However, this kind of electrolyte can flow using low-viscosity ionic liquid such as 1-butyl-3-methylimidazolium iodide (BMI·I) and SiO_2 nanoparticles with low specific surface area (such as Aesoil 200). Herein, we modified the experiments by introducing the anion tetrafluoroborate (BF_4^-). Interestingly, the flow mixture of BMI·I and SiO_2 was solidified successfully by incorporating BF_4^- (Figure 1). We deduced that the BF_4^- anion played an important role in the process of solidification and promoted readily this solid-state mixture. Furthermore, such a solid was employed as an additive to fabricate a novel high temperature (>85°C) solid-state nanocomposite (SNC) electrolyte for dye-sensitized solar cells. Importantly, the solid-state DSSC based on the SNC electrolyte exhibits a high overall energy conversion efficiency of 5.0% at 60 °C.

Experimental Section

Materials and Instruments. Titanium(IV) tetraisopropoxide and 4-*tert*-butylpyridine were purchased from Acros. Fumed silica (Aesoil 200, 12 nm) was received as a gift from Degussa Company. 1-Butyl-3-methylimidazolium tetrafluoroborate (BMI·BF_4) and other chemicals (Sinopharm Chemical Reagent Co., Ltd, Shanghai, China) were used without further purification. 1-Butyl-3-methylimidazolium iodide (BMI·I) was synthesized according to the literature.[19] *cis*-Dithiocyanato-*N*,*N*-bis(2,2′-bipyridyl-4,4′-dicarboxylic acid)ruthenium(II) (N3) was purchased from Solaronix, Switzerland. The 120 g L^{-1} TiO_2 colloidal was prepared according to the literature.[20]

The ionic conductivity of the electrolytes was determined by an ac impedance technique (frequency range: 1 Hz to 1 MHz) using an impedance/gain-phase analyzer (Solartron SI 1255B) connected with a potentiostat (Solartron SI 1287). The ac voltage was fixed at 0.005 V. The current−voltage (*I*−*V*) characteristics of the solar cells were carried out using a Keithley 2400 Source Meter. An AM 1.5 solar simulator (Oriel Instruments, 91193 with a 1000W Xe lamp and an AM 1.5 filter) was employed as the light source. The incident light intensity was calibrated with a standard Si solar cell. Fourier transition infrared (FT-IR) measurements were performed on American Nicolet Company, Nexus 470 FT-IR spectrometer. Differential scanning calorimetry (DSC) was studied on a Shimazu DSC-60A. The 10 mg samples were taken at a heating rate of 10 °C min^{-1} in a temperature range of 25−250 °C.

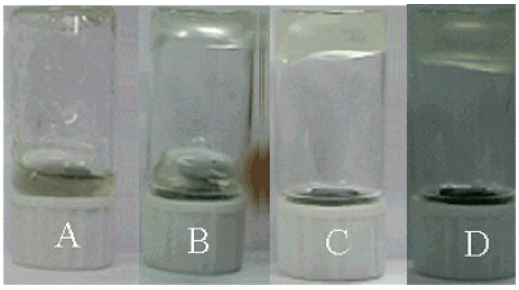

Figure 2. Photographs of BMI·BF_4−SiO_2 system with different contents of silica nanoparticles: 1 wt % (A), 2 wt % (B), 3 wt % (C), and 4 wt % (D).

Preparation of Electrolytes. Herein, the liquid electrolyte was composed of 0.18 M I_2, 1.3 M BMI·I, 0.5 M LiI, and 1 M 4-*tert*-butylpyridine in BMI·BF_4. An amount (1−6 wt %) of silica nanoparicles was added to the liquid electrolyte to form nanocomposite (NC) electrolytes. In the process of preparing, no evaporable organic solvent was introduced. To improve homogeneity, the mixture was sonicated and then stirred vigorously for 12 h.

Preparation of Solar Cells. DSSCs with an active area of 0.188 cm^{-2} were fabricated according to the following procedure. The colloidal solution was spread uniformly on the conducting CTO glass and then sintered at 450 °C in airflow for 30 min. The resultant TiO_2 films were immersed in 0.5 mM absolute ethanol solution of N3 for 1 day. The nanocomposite (NC) electrolyte with 5 wt % SiO_2 nanoparticles was spin-coated onto the N3-absorbed TiO_2 electrode and kept in the vacuum oven for 2 h. The counter electrode was sputtered by 200 nm thick Pt on the CTO glass. Subsequently, the cells were sealed with thermal adhesive films (Surlyn 1702).

Results and Discussion

Figure 2 shows the photographs of the ionic liquid BMI·BF_4 blended with different contents of SiO_2 nanoparticles with low specific surface area (Aesoil 200). It can be found from Figure 2 that BMI·BF_4 could be solidified by SiO_2 nanoparticles. Especially, the solid-state composite was completely formed by adding greater than 2 wt % of SiO_2 nanoparticles. However, no obvious solidification was observed for the mixture of BMI·I and silica nanoparicles (Aesoil 200) even if the weight of silica nanoparticles reached 6 wt %.

To understand the mechanism of the solidification, we compared the mixture of BMI·BF_4 and SiO_2 nanoparticles (5 wt %) (BMI·BF_4−SiO_2) with the mixture of BMI·I and SiO_2 nanoparticles (5 wt %) (BMI·I−SiO_2) by differential scanning calorimetry (DSC) measurement and FT-IR spectra. The DSC thermogram of BMI·BF_4−SiO_2 shows an endothermic peak centered around 171.7 °C (Figure 3.). This endothermic peak reveals that crystalline regions are formed in the composite, which melt at the temperature of 171.7 °C. Below this temperature the composite remains solid. The

(16) (a) Wang, P.; Zakeeruddin, S. M.; Humphry-Baker, R.; Grätzel, M. *Chem. Mater.* **2004**, *16*, 2694. (b) Wang, P.; Zakeeruddin, S. M.; Moser, J. E.; Humphry-Baker, R.; Grätzel, M. *J. Am. Chem. Soc.* **2004**, *126*, 7164. (c) Wang, P.; Wenger, B.; Humphry-Baker, R.; Moser, J. E.; Teuscher, J.; Kantlehner, W.; Mezger, J.; Stoyanov, E. V.; Zakeeruddin, S. M.; Grätzel, M. *J. Am. Chem. Soc.* **2005**, *127*, 6850, and references therein.
(17) (a) Kubo, W.; Kitamura, T.; Hanabusa, K.; Wada, Y.; Yanagida, S. *Chem. Commun.* **2002**, 374. (b) Mohmeyer, N.; Wang, P.; Schmidt, H. W.; Zakeeruddin, S. M.; Grätzel, M. *J. Mater. Chem.* **2004**, *14*, 1905. (c) Stathatos, E.; Lianos, P.; Vuk, A. S.; Orel, B. *Adv. Funct. Mater.* **2004**, *14*, 45.
(18) Wang, P.; Zakeeruddin, S. M.; Comte, P.; Exnar, I.; Grätzel, M. *J. Am. Chem. Soc.* **2003**, *125*, 1166.
(19) Bonhte, P.; Dias, A. P.; Armand, M.; Papageorgiou, N.; Kalyanasudaram, K.; Grätzel, M. *Inorg. Chem.* **1996**, *35*, 1168.
(20) Nazeeruddin, M. K.; Kay, A. R.; Humphry-Baker, I.; Mueller, R.; Liska, E.; Vlachopoulos, P. N.; Grätzel, M. *J. Am. Chem. Soc.* **1993**, *115*, 6382.

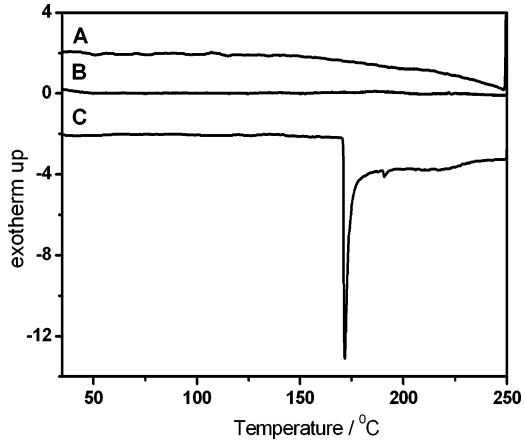

Figure 3. DSC thermograms of BMI·BF_4 (A), BMI·I−SiO_2 (B), and BMI·BF_4−SiO_2 (C).

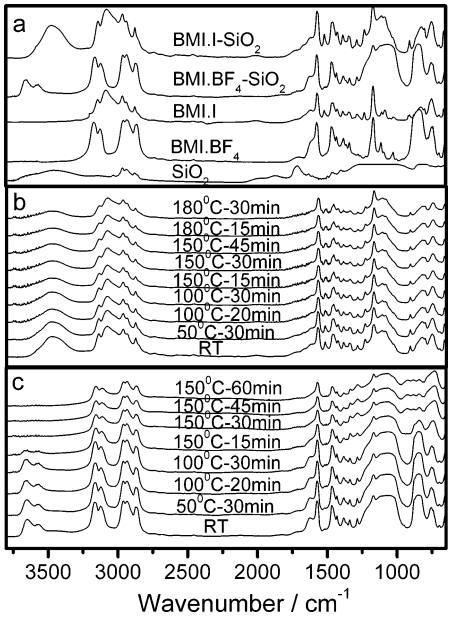

Figure 4. FT-IR spectra of BMI·I, SiO_2, BMI·BF_4, BMI·I−SiO_2 (5 wt %) and BMI·BF_4−SiO_2 (5 wt %) at room temperature (a); BMI·I−SiO_2 (5 wt %) at different temperature (b); BMI·BF_4−SiO_2 (5 wt %) at different temperature (c).

change in enthalpy (ΔH) was −17.2 J g^{-1}. However, no peak was observed below 250 °C for both BMI·BF_4 and BMI·I−SiO_2. Accordingly, this peak may be attributed to the breakage of the strong interaction between silica nanoparicles and tetrafluoroborate, not phase transition of BMI·BF_4 or silica nanoparicles.[21]

Figure 4 shows the FT-IR spectra of BMI·BF_4−SiO_2 and BMI·I−SiO_2 at different temperatures. For comparison, the FT-IR spectra of SiO_2, BMI·I, and BMI·BF_4 are also shown in Figure 4a, and no vibration bands beyond 3500 cm^{-1} were observed for BMI·I and BMI·BF_4. The FT-IR spectrum of the silica nanoparicles showed a broad peak at 3478 cm^{-1}, which was attributed to the hydrogen-bonded chains of silanols.[22] When the silica nanoparticles mixed with BMI·I, the broad vibration band peaked at ∼3500 cm^{-1} was observed. Such a little shift (20 cm^{-1}) of the hydrogen-bonded chains of silanols suggested a weak interaction between BMI·I and SiO_2. In contrast, the vibration bands at 3648 and 3572 cm^{-1} were observed for BMI·BF_4−SiO_2, indicating the anion BF_4^- had the stronger interaction with the hydroxyl group of silanols. This fact indicated that the different nature of anions may be responsible for the observed phenomena. Because of the strong electronegativity of the F atom, BMI·BF_4 may disturb hydrogen-bonded pairs or chains of silanols significantly; hence, the vibration band of 3478 cm^{-1} disappeared. The temperature dependencies of the FT-IR spectra of these two systems were also investigated (Figures 4b and 4c). The vibration bands at 3648 and 3572 cm^{-1} became weaker with increasing of the treatment temperature and completely disappear when the temperature was above 150 °C. In contrast, no obvious change in FT-IR spectra of the BMI·I−SiO_2 system was observed even at elevating treatment temperature, which indicated the interaction between I^- and silanol was very weak. The above observations may also suggest that the strong interaction mainly occurs between silica nanoparticles and the anion BF_4^-, not between silica nanoparticles and the imidazium cation. Therefore, the solidification most likely originates from the self-assembly of hydrogen bonds between the OH group of silica nanoparicles and the F atom of BF_4^-, due to the strong electronegativity of the F atom.

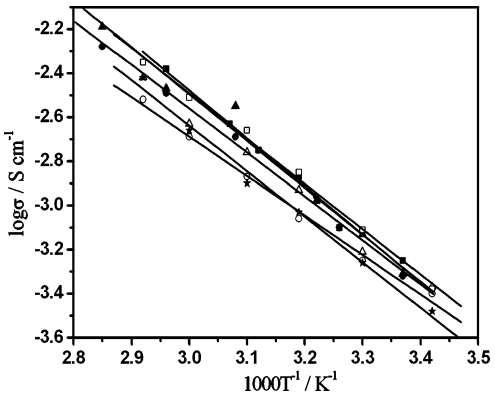

Figure 5. Ionic conductivity as a function of temperature for the liquid electrolyte (■) and composite electrolytes upon the addition of 1 wt % (●), 2 wt % (▲), 3 wt % (△), 4 wt % (□), 5 wt % (○), and 6 wt % (∗) silica nanoparicles.

Generally, the overall energy conversion efficiency of DSSC is heavily dependent upon the mobility of the redox couple (I^-/I_3^-) and consequently on the ionic conductivity of the electrolyte.[23] In this regard, the solid-state nanocomposite (SNC) electrolyte was fabricated using the mixture of BMI·BF_4 and SiO_2 nanoparticles as the additive, and the ionic conductivity was studied. To optimize the added quantity of silica nanoparicles, the ionic conductivity of the composite electrolytes with various SiO_2 weight percent (1−6 wt %) was investigated as a function of temperature (Figure 5). The ionic conductivity shows a linear dependence on the temperature, indicating typical Arrenius behavior.[18] Compared to the liquid electrolyte, the composite electrolytes show no obvious decrease of the ionic conductivity within the measured temperature range (25−100 °C). According

(21) Holdon, G. *Thermoplastic Elastomers* [M]; Academic Press Inc.: New York, 2000.
(22) Morrow, B. A.; McFarlan, A. J. *J. Phys. Chem.* **1992**, *96*, 1395.
(23) Kubo, W.; Murakoshi, K.; Kitamura, T.; Yoshida, S.; Haruki, M.; Hanabusa, K.; Shirai, H.; Wada, Y.; Yanagida, S. *J. Phys. Chem. B* **2001**, *105*, 12809.

Figure 6. Photograph of the SNC electrolyte (0.18 M I_2, 1.3 M BMI·I, 0.5 M LiI, 1 M 4-*tert*-butylpyridine in BMI·BF_4, 5 wt % silica nanoparicles) at 85 °C.

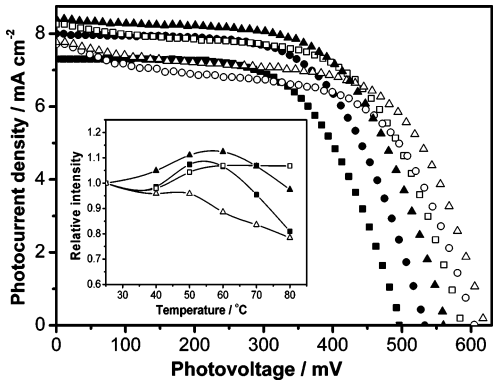

Figure 7. *J*−*V* curves for the solar cell based on the SNC electrolyte at different temperatures. 25 °C (△), 40 °C (○), 50 °C (□), 60 °C (▲), 70 °C (●), and 80 °C (■). Inset: the relation of performance of the cell with different temperatures, η (■), FF (□), J_{sc} (▲), and V_{oc} (△).

to the Arrenius equation, the activation energy data of these composite electrolytes (14.9−17.7 kJ mol^{-1}) is slightly lower than that of the liquid electrolyte (18.1 kJ mol^{-1}). Moreover, all composite electrolytes exhibit high ionic conductivity of $\sim 4.0 \times 10^{-4}$ S cm^{-1} at 19 °C and $>10^{-3}$ S cm^{-1} at 60 °C. These results suggest that the above composite electrolytes should be good candidates as high-temperature electrolytes in DSSCs. It is noteworthy that the nanocomposite electrolytes are solid state when the concentration of silica nanoparicles added to the liquid electrolyte is greater than 2 wt %. Considering the solidification effect and optimum ionic conductivity, we selected the nanocomposite electrolyte with 5 wt % silica nanoparicles to fabricate a solid-state DSSC. As shown in Figure 6, this nanocomposite electrolyte (0.18 M I_2, 1.3 M BMI·I, 0.5 M LiI, 1 M 4-*tert*-butylpyridine in BMI·BF_4, and 5 wt % silica nanoparicles) can still maintain solid state at a high temperature (>85 °C). Herein, this composite electrolyte was denoted as the SNC electrolyte.

Since the working temperature of DSSC is expected to be considerably greater than room temperature, the temperature dependence of the cell performances was investigated to check the possibility of DSSC working at higher temperature. Figure 7 shows the parameters for the cell made with the SNC electrolyte in the temperature range of 25−80 °C. Open-circuit voltage (V_{oc}) decreases almost linearly with increasing temperature. A drop in V_{oc} is considered to be

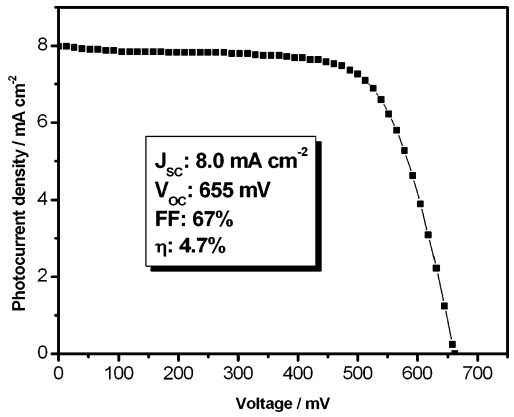

Figure 8. *J*−*V* curve of the cell made with SNC electrolyte.

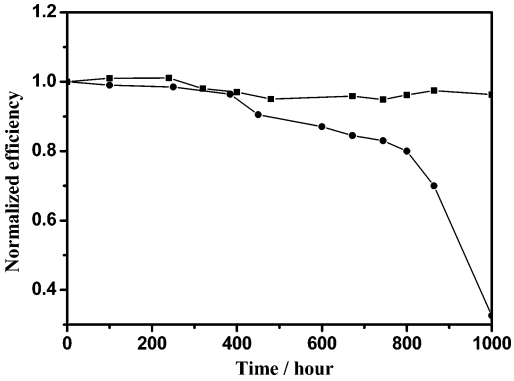

Figure 9. Time-course change of the normalized photoconversion efficiency of the liquid electrolyte (●) and SNC electrolyte (■).

the different recombination energy.[24] Short-circuit current density (J_{sc}) rises quickly with an increase of the temperature and achieves a maximum value when the operation temperature reaches 60 °C in accordance with the conductivity data. We also observe that a maximum value of the overall energy conversion efficiency (η) appears around 50 °C, resulting from the relation with short-circuit current density and open-circuit voltage. These facts indicate that the cell can work well under elevated temperature. The high ionic conductivity of the SNC electrolyte and good interfacial contact can improve the efficiency of DSSC. The optimum results at room temperature for the cell using SNC electrolyte are 8.0 mA cm^{-2} of J_{sc}, 655 mV of V_{oc}, 67% of FF, and 4.7% of η (see Figure 8), which is a very encouraging value for a solid-state DSSC.[7b,9] More importantly, at the relatively high temperature of 60 °C, the solar cell based on the SNC exhibits 5.0% of overall energy conversion efficiency, which is one of the highest values in all reported solid-state DSSCs worked at 60 °C up to now.[25]

To investigate the long-time practical stability of these solid-state DSSCs, herein, the aging test on the cells sealed with thermal adhesive films (Surlyn 1702) according to the literature[23] was carried out. The cells were stored at 60 °C for 1000 h, and their photoconversion efficiency was measured twice a week. As expected, no decrease of the

(24) Kron, G.; Egerter, T.; Nellesb, G.; Yasudab, A.; Werner, J. H.; Rau, U. *Thin Solid Films* **2002**, *403*−*404*, 242.
(25) (a) Schmidt-Mende, L.; Zakeeruddin, S. M.; Grätzel, M. *Appl. Phys. Lett.* **2005**, *86*, 013504. (c) Kim, J. H.; Kang, M. S.; Kim, Y. J.; Won, J.; Park, N. G.; Kang, Y. S. *Chem. Commun.* **2004**, 1662.

efficiency was observed for the solid-state DSSCs at all, while the efficiency of the liquid DSSCs maintained only 30% of their initial efficiency after 1000 h (Figure 9). A possible reason for the higher stability of the solid-state solar cells is the exclusion of water from the SNC electrolyte in the presence of interaction between the hydroxyl group of silanols and the anion BF_4^- with relatively hydrophilic property.[26] It is possible that the high-temperature stability of SNC electrolytes composed of RTIL and silica nanoparticles provide the practical efficiency and stability of the DSSCs.

Conclusion

In summary, a high-temperature solid-state nanocomposite (SNC) electrolyte was designed for application in DSSCs. By introduction of the self-assembly of hydrogen bonds networks formed with the anion BF_4^- and silica nanoparticles, the solid nanocomposite electrolyte was fabricated and exhibited good ionic conductivity. As a result, the solid-state cell based on the SNC electrolyte exhibited an encouraging overall efficiency of 4.7% (75 mW cm^{-2}) at room temperature. Importantly, the nanocomposite electrolyte maintained solid state even up to 85 °C and showed long-time stability with a high overall efficiency of 5.0% at 60 °C. The result provides a useful design strategy for high-temperature solid-state electrolytes for further application.

Acknowledgment. The authors thank the National Science Foundation of China (20490210 and 20501006), National 863 Program of China (2002AA302403), Huo Yingdong Education Foundation (104012), and Shanghai Science and Technology Committee (05DJ14004) for financial support.

CM061112D

(26) Lee, B. S.; Chi, Y. S.; Lee, J. K.; Choi, I. S.; Song, C. E.; Namgoong, S. K.; Lee, S. G. *J. Am. Chem. Soc.* **2004**, *126*, 480.